



Published in final edited form as:

Nature. 2010 June 24; 465(7301): 1079–1083. doi:10.1038/nature09118.

Subcapsular Sinus Macrophages Prevent CNS Invasion Upon Peripheral Infection With a Neurotropic Virus

Matteo Iannacone^{1,4,5}, E. Ashley Moseman^{1,5}, Elena Tonti¹, Lidia Bosurgi¹, Tobias Junt², Sarah E. Henrickson¹, Sean P. Whelan³, Luca G. Guidotti⁴, and Ulrich H. von Andrian¹

¹ Immune Disease Institute and Department of Pathology, Harvard Medical School, 77 Ave Louis Pasteur, Boston, MA 02115, USA ² Novartis Institutes for BioMedical Research, 4002 Basel, Switzerland ³ Department of Microbiology and Molecular Genetics, Harvard Medical School, 200 Longwood Avenue, Boston, MA 02115, USA ⁴ Department of Immunology, Infectious Diseases and Transplantation, San Raffaele Scientific Institute, Via Olgettina 58, Milan, 20132 Italy

Abstract

Lymph nodes (LNs) capture microorganisms that breach the body's external barriers and enter draining lymphatics, limiting the systemic spread of pathogens¹. Recent work has shown that CD11b⁺CD169⁺ macrophages, which populate the subcapsular sinus (SCS) of LNs, are critical for clearance of viruses from the lymph and for initiating antiviral humoral immune responses^{2,3,4}. Using vesicular stomatitis virus (VSV), a relative of rabies virus transmitted by insect bites, we show here that SCS macrophages perform a third vital function: they prevent lymph-borne neurotropic viruses from infecting the CNS. Upon local depletion of LN macrophages, ~60% of mice developed ascending paralysis and died 7–10 days after subcutaneous infection with a small dose of VSV, while macrophage-sufficient animals remained asymptomatic and cleared the virus. VSV gained access to the nervous system via peripheral nerves in macrophage-depleted LNs. In contrast, within macrophage-sufficient LNs VSV replicated preferentially within SCS macrophages but not in adjacent nerves. Removal of SCS macrophages did not compromise adaptive immune responses against VSV, but reduced type I interferon (IFN-I) production within infected LNs. VSV-infected macrophages recruited IFN-I producing plasmacytoid dendritic cells to the SCS and additionally were a major source of IFN-I themselves. Experiments in bone marrow chimeric mice revealed that IFN-I must act on both hematopoietic and stromal compartments, including the intranodal nerves, to prevent lethal VSV infection. These results

Users may view, print, copy, download and text and data- mine the content in such documents, for the purposes of academic research, subject always to the full Conditions of use: http://www.nature.com/authors/editorial_policies/license.html#terms

Address correspondence to: Ulrich H. von Andrian, M.D. (uva@hms.harvard.edu) or Matteo Iannacone, M.D. (Matteo_Iannacone@hms.harvard.edu or matteo@iannacone.org) Dept. of Pathology, Harvard Medical School, 77 Ave. Louis Pasteur, Boston, MA 02115. Phone: (617) 432-6827; Fax: (617) 432-6829.

⁵These authors contributed equally to this work.

Author contribution.

M.I., E.A.M. and U.H.v.A. designed the study; M.I., E.A.M., E.T., L.B. and T.J. performed experiments; M.I., E.A.M., E.T. and L.B. collected and analyzed data; S.P.W. provided reagents and performed RT-PCR experiment; S.E.H. contributed to the nerve imaging; L.G.G. provided mice and gave conceptual advice; M.I., E.A.M. and U.H.v.A. wrote the manuscript; M.I. and E.A.M. contributed equally to this work.

identify SCS macrophages as crucial gatekeepers to the CNS that prevent fatal viral neuroinvasion upon peripheral infection.

To explore how neurotropic viruses spread from their entry site to the CNS, we studied VSV, an arthropod-borne rhabdovirus that causes fatal paralytic disease in mammals, including mice⁵. While numerous studies have investigated immune responses to intravenous VSV infection⁶, the immunological consequences elicited by the more natural subcutaneous (sc) route are incompletely understood. Previous work has shown that, following peripheral inoculation, VSV is captured by macrophages in draining LNs, preventing hematogenous dissemination². Here, we asked whether this macrophage filter affects the ability of neurotropic viruses to access the CNS.

C57BL/6 mice were injected sc with clodronate liposomes (CLL) into one hind footpad, which selectively eliminated CD11b⁺CD169⁺ macrophages in the draining popliteal LN, but not in distal LNs or the spleen². Six days later, mice were challenged in the ipsilateral or contralateral footpad using a low dose (10⁴ pfu) of VSV-Indiana. While this dose was cleared by virtually all untreated and contralaterally-infected mice, ~60% of CLL-treated ipsilaterally-infected animals developed ascending CNS pathology starting with ipsilateral hindleg paralysis and progressing to death 7–10 days after infection (Fig. 1a). Equivalent results were obtained using Balb/c mice or VSV-New Jersey (Suppl. Fig. 1). CLL-dependent susceptibility to fatal neuropathology was a direct consequence of viral CNS invasion, since infectious virus and virus-induced pathology became detectable in the brain (Fig. 1b) and spinal cord (Suppl. Fig. 2) exclusively in symptomatic CLL-treated mice.

To confirm that CLL promoted VSV neuroinvasion through macrophage depletion and not by other mechanisms, we sought an alternative approach to eliminate LN-resident macrophages. LN macrophages express moderate levels of CD11c² and are susceptible to the toxic effects of diphtheria toxin (DT) in CD11c-DTR mice⁷. Indeed, footpad injection of DT eliminated CD169⁺ LN macrophages in the draining LN, while leaving paracortical CD11c⁺ dendritic cells unchanged (Suppl. Fig. 3). DT treatment rendered CD11c-DTR mice susceptible to fatal VSV infection with a clinical course and mortality similar to CLL-treated animals (Fig. 1c). These results, based on two mechanistically distinct approaches, indicate that CLL-sensitive CD11c⁺ phagocytes are essential for neuroprotection following peripheral VSV infection.

To pinpoint the site of viral susceptibility, we considered four candidate access routes for viral neuroinvasion following sc infection in CLL-treated mice: (1) direct entry across the blood-brain barrier either by free circulating virions⁸ or (2) by virus-bearing migratory cells or (3) entry via peripheral nerves in the infected footpad and/or (4) the draining LNs.

Following sc VSV deposition, viral particles rapidly drain to regional LNs where macrophages capture lymph-borne virions². Since CLL eliminates this macrophage filter, infectious virions can reach the blood via efferent lymphatics². However, at the low VSV dose (10⁴ pfu) used here, we did not detect a ‘spillover’ of infectious virus in blood (Suppl. Fig. 6c). Moreover, CLL-treated animals survived intravenous injections of 10⁴ pfu VSV (Fig. 1d), consistent with earlier reports that the median lethal dose for i.v. injected VSV is

~10⁸ pfu in C57BL/6 mice⁹. Therefore, hematogenous dissemination seemed an unlikely pathway for infectious virions to access the CNS. However, it remained theoretically possible that migratory cells infected in the hindleg acted as “Trojan horses” by transporting VSV via the blood into the CNS. To distinguish between this candidate pathway and the alternative access route, peripheral nerves in the hindleg, we resected sciatic nerves in CLL-treated mice prior to VSV infection. Indeed, ipsilateral denervation, but not contralateral or sham denervation, protected CLL-treated mice against VSV neuroinvasion (Fig. 1e), indicating that VSV does not enter the CNS hematogenously, but through distal branches of the sciatic nerve within anatomic regions that contain CLL-sensitive CD11c⁺ phagocytes and that are directly exposed to VSV as well as CLL, i.e. the footpad and/or the draining LNs.

Since the CLL injection site developed a myeloid infiltrate during the first week (Fig. 1f), we asked whether this inflammatory response might enhance the susceptibility of nearby nerves to VSV injected into the same site. Thus, we modified our approach such that the only CLL-exposed (and hence macrophage-depleted) environment encountered by VSV was the popliteal LN. Because this LN receives lymph from the entire lower leg, we could deplete LN-resident CD11b⁺CD169⁺ macrophages by sc injection of CLL into the calf while leaving the footpad unaffected (Fig. 1f and Suppl. Fig. 4a,b). When VSV was injected into essentially normal footpads, mice treated with CLL in the calf recapitulated the increased mortality observed when both injections were given in the footpad (Fig. 1g). Mice also remained susceptible to VSV neuroinvasion when they were infected 60 days after CLL footpad injection (Suppl. Fig. 4c). At this time point, the inflammatory infiltrate in the footpad had resolved, while LN macrophages remained depleted (Suppl. Fig. 4d,e)¹⁰. We conclude that VSV-draining LNs are the principal sites of viral neuroinvasion, and LN macrophages are critical mediators of neuroprotection.

To visualize viral replication, we infected macrophage-sufficient mice with VSV-eGFP, which drives GFP expression selectively within infected cells¹¹. Consistent with a recent report¹², VSV replicated selectively in LN macrophages (Fig. 2a,b), however, viral replication was anatomically restricted; only CD169^{hi} SCS macrophages were GFP⁺, while CD169^{dim} medullary macrophages showed no evidence of viral replication (Fig. 2a and Suppl. Fig. 5). Accordingly, when macrophage-depleted animals were infected with VSV-eGFP, draining LNs were almost completely devoid of GFP⁺ cells (Fig. 2c and Suppl. Fig. 5).

To locate peripheral nerves in popliteal LNs, we stained popliteal LNs for β 3-tubulin, which revealed a branched network of peripheral nerves in the capsule and SCS (Fig. 2d and Suppl. Movies 1&2). In VSV-eGFP-infected control animals, these nerves were surrounded by infected (i.e. GFP⁺) SCS macrophages, but the nerves themselves showed little evidence of VSV replication (Fig. 2e). In contrast, in macrophage-depleted LNs, VSV-eGFP replicated within nerves in and around the SCS. Indeed, the GFP signal colocalized exclusively with β 3 tubulin, indicating that VSV replicated selectively in nerves and no other cell types (Fig. 2f,g).

Having established that SCS macrophages protect peripheral nerves against viral neuroinvasion, we investigated three plausible, non-exclusive mechanisms for this vital function: 1) macrophages might phagocytose and destroy viral particles; 2) they might promote adaptive antiviral immune responses; or 3) they might exert innate immune activities thwarting viral entry or replication in nerves. Because SCS macrophages actively replicate VSV (Fig. 2a,b,e), direct macrophage-mediated viral destruction seemed doubtful. Indeed, viral titers were much higher in macrophage-sufficient popliteal LNs than in CLL-treated LNs during the first 36h after infection (Fig. 2h). Both groups had similarly low viral titers in downstream inguinal LNs (Suppl. Fig. 6a), and VSV was never detectable in the spleen or blood (Suppl. Fig. 6b,c). Thus, SCS macrophages actually boosted the overall viral burden, presumably by providing a preferred substrate for VSV replication, which is at odds with the idea that these cells prevent viral neuroinvasion by destroying infectious virions.

Previous work had identified SCS macrophages as critical initiators of B cell activation in LNs^{2,3,4}, and humoral immunity is considered essential for VSV clearance^{13,14}. However, the neutralizing antibody response in macrophage-depleted mice was not impaired, but rather enhanced as compared to control animals (Fig. 2i). Similarly, both CD4 and CD8 T cell responses were normal or even greater in macrophage-depleted mice (Suppl. Fig. 7). Thus, CLL-mediated removal of LN macrophages does not compromise adaptive immunity to peripheral infection with low-dose VSV. In fact, even though SCS macrophages are needed to initiate B cell activation during the first 6 hours after VSV challenge², the overall VSV-specific adaptive immune response was enhanced one week after CLL treatment. This may have been due, at least in part, to increased trafficking of antigen-presenting dendritic cells from the inflamed CLL-treated footpad to the draining LN (not shown).

Although CLL-treated mice mounted a supranormal adaptive response to VSV, the majority nevertheless succumbed to VSV-induced neuropathology (Fig. 1a and Suppl. Fig 2b,d), indicating that adaptive immunity is insufficient for protection, at least in settings that mimic the natural route and dose of VSV infection. CLL-sensitive LN macrophages apparently make essential contributions to antiviral immunity by one or more innate immune mechanisms. Type I interferon (IFN-I) is critical in many viral infections, including VSV⁹. Strikingly, upon VSV infection macrophage-depleted LNs contained ~90% less IFN α than control LNs (Fig. 3a). Accordingly, mRNA levels of interferon-inducible genes, such as OAS and ISG15, were reduced after macrophage depletion (data not shown).

Next, we asked how macrophage depletion compromised VSV-induced IFN-I production. Conceivably, infected SCS macrophages could produce the cytokine. Alternatively, they could indirectly stimulate IFN-I release by other cells, such as plasmacytoid dendritic cells (pDCs), which recognize VSV through Toll-like receptor (TLR)7 and represent a major source of IFN-I in many conditions^{15,16}. The number of LN-resident pDCs was not affected by CLL treatment (Suppl. Fig. 8a,b) and, unlike SCS macrophages, pDCs were not productively infected by VSV (Suppl. Fig. 8c). However, when pDCs were depleted prior to VSV infection (Suppl. Fig. 8b) IFN α levels were 52 \pm 0.9% lower than in pDC-sufficient controls (Fig. 3a). Moreover, combined depletion of both pDCs and macrophages abolished IFN α production (96 \pm 0.7% reduction). Thus, while pDCs produce IFN α upon sc VSV infection, ~half of the IFN-I is contributed by CLL-sensitive non-pDCs.

To determine whether VSV induces IFN-I production by SCS macrophages, we infected mice with VSV-eGFP and FACS-sorted GFP⁺ infected macrophages and GFP⁻ non-infected LN cells 4h later (Suppl. Fig. 9a). After culturing equivalent numbers of sorted cells, infected macrophage supernatant contained ~4-fold more IFN α than non-infected cells supernatant (Fig. 3b). Although the non-infected population contained IFN α -producing pDCs, the detected IFN α concentration was low presumably because pDCs are relatively rare among the multitude of other GFP⁻ cells. Indeed, when we compared GFP⁺ SCS macrophages against sorted CD11c⁺GFP⁻ DCs (Suppl. Fig. 9b), the two cell populations produced similar amounts of IFN α (Fig. 3c). These *in vitro* results fit well with our *in vivo* findings in cell-depleted LNs and establish infected SCS macrophages and pDCs as the two critical sources of VSV-induced IFN-I in peripheral LNs. The relative contribution of other cell types, such as medullary macrophages, to IFN-I production remains to be determined.

Of note, CLL-induced macrophage depletion alone reduced IFN α production almost as efficiently as combined depletion of pDCs and macrophages together (Fig. 3a), suggesting that LN macrophages are required for IFN-I production by pDCs. Because pDCs are not infected themselves (Suppl. Fig. 8c), they must localize to LN areas where viral material is accessible for detection by TLR7. Thus, we speculated that macrophages recruit pDCs to the medulla and SCS where macrophages capture and retain lymph-borne virions². To visualize pDCs, we transplanted mixed bone marrow (BM) from wildtype and DPE-GFPxRAG2^{-/-} mice¹⁷ into irradiated wildtype recipients to generate mixed BM chimeras in which ~30% of LN pDCs were GFP⁺ (Suppl. Fig. 10). In steady-state LNs, most pDCs were located in the T cell zone with the remainder in the medulla and peri-follicular area (Fig. 3d-i), whereas pDCs were rarely found in the SCS. Upon infection, pDCs peripheralized from the deep cortex towards the SCS and medulla. However, following macrophage depletion, pDCs in VSV-infected LNs did not depart from the T cell area and remained scarce in the SCS (Fig. 3g-i and Suppl. Figs. 11,12). These results suggest that interactions of LN macrophages with VSV lead to pDC relocalization to the site of viral capture and/or infection, presumably due to the release of unidentified chemoattractants. Additionally, it is conceivable that virus-exposed macrophages prevent pDC egress into efferent lymph, thus promoting pDC retention in sinus-proximal regions.

In contrast to macrophage depletion, antibody depletion of pDCs prior to VSV infection did not result in increased mortality in either control or macrophage-depleted mice (Fig. 3j), suggesting that the localized IFN-I production by SCS macrophages alone is neuroprotective. IFN-I from pDCs appears dispensable for survival after VSV, but may contribute to other aspects of antiviral immunity, like the development of adaptive responses.

Having determined that macrophage-derived IFN-I is critical, we asked where IFN-I must act to prevent neuroinvasion. We made use of IFN-I receptor-deficient (IFN $\alpha\beta$ R^{-/-}) mice, which are exquisitely sensitive to VSV infection⁹; following VSV footpad infection, these animals succumbed rapidly within 4–5 days (Fig. 3k), however, without developing the ascending paralysis observed in CLL-treated wild-type mice. To characterize this difference in disease progression, we generated BM chimeras that lacked IFN $\alpha\beta$ R in either hematopoietic or non-hematopoietic cells. Upon sc infection, mice lacking hematopoietic

IFN α β R recapitulated the phenotype of IFN α β R^{-/-} mice, dying abruptly after 4–5 days without developing ascending paralysis (Suppl. Fig. 13a). By contrast, mice lacking stromal (including peripheral nerve) IFN α β R exhibited slowly ascending CNS pathology, starting with ipsilateral hindlimb paralysis, resembling the disease in macrophage-depleted wild-type mice. Interestingly, viral replication was always restricted to SCS macrophages when hematopoietic cells expressed IFN α β R, while mice lacking hematopoietic IFN α β R replicated VSV also in other LN cells (Suppl. Fig. 13b–e). By contrast, macrophage depletion in LNs containing IFN α β R-sufficient hematopoietic cells did not result in enhanced or aberrant viral replication in LN cells other than peripheral nerves (Fig. 2f,g), indicating that the residual IFN-I produced in CLL-treated wild-type animals is sufficient to protect hematopoietic but not stromal cells.

Based on these results, we can reconstruct the chain of events that ensues following subcutaneous deposition of VSV: initially, viral particles enter local lymphatics and are transported to draining LNs. Here, two macrophage populations, one in the SCS the other in the medulla, capture and retain lymph-borne virions². While medullary macrophages do not replicate VSV, SCS macrophages replicate the virus and secrete IFN-I. VSV capture by both macrophage subsets triggers production of unidentified chemoattractant(s) for pDC, which migrate from the deep cortex toward the SCS and medulla where they encounter VSV and produce additional IFN-I. A modest amount of macrophage-independent IFN-I is sufficient to protect other hematopoietic LN cells. Higher concentrations and/or localized production of IFN-I are required to prevent viral replication in LN peripheral nerves. Neuroprotective concentrations of IFN-I are only achieved when SCS macrophages are present (and presumably infected by VSV). It remains to be determined whether IFN-I exerts its protective function by preventing viral entry into or replication within peripheral nerves or the CNS¹⁸, and whether IFN-I acts on neurons or on accessory cells, such as Schwann cells. It will be relevant to explore the clinical implications of our findings, particularly for rabies infections and other arthropod-borne neurotropic viruses, such as West Nile virus⁸.

Method Summary

C57BL/6, BALB/c, CD11c-DTR GFP¹⁹, Tg7²⁰, DPE-GFP²¹, and IFN α β R^{-/-9} mice were used. VSV, serotypes Indiana (Mudd-Summers derived clone, in vitro rescued²² and plaque purified), New Jersey (Pringle Isolate, plaque purified), and VSV-eGFP¹¹ were propagated on BSRT7 cells, and purified as described². LN macrophages were depleted by injections in the footpad or in the calf of clodronate liposomes (CLL²³) or diphtheria toxin 6 days or 60 days prior to infection. In other experiments pDCs were depleted by intravenous injection of anti-PDCA-1 MAb 24h prior to infection. VSV titers from organs of infected mice were determined by plaque assay on Vero cells. Serum of infected or control mice was assessed for the presence of neutralizing antibody titers as described². After footpad infection, draining popliteal LNs were harvested for whole mount immunofluorescence multiphoton microscopy analysis, for flow cytometry analysis, or to generate frozen sections for immunostaining and confocal microscopy. LN protein extracts and supernatants from sorted VSV-infected cells were assayed for IFN α using an IFN α ELISA kit (PBL InterferonSource). For sciatic nerve resection, the nerve was exposed through an incision on the lateral aspect of the mid thigh, resected and the distal and proximal nerve stumps were

separately tucked into adjacent intermuscular spaces to prevent nerve regeneration. Results are expressed as mean \pm s.e.m. Means between two groups were compared using two-tailed *t*-test. Means among three or more groups were compared using one-way analysis of variance with Bonferroni's post-test. Kaplan-Meier survival curves were compared using the Log-rank (Mantel-Cox) test.

Supplementary Material

Refer to Web version on PubMed Central for supplementary material.

Acknowledgments

We thank G. Cheng and M. Flynn for technical support; J. Alton for secretarial assistance; D. Cureton for help and advice with VSV preparations; H. Leung for help with image quantification; R. M. Zinkernagel and H. Hengartner for providing tg7 mice; R. Bronson for help reading neuropathology; S. Cohen for advice on nerve staining; and the members of the von Andrian lab for helpful discussion. This work was supported by NIH grants AI069259, AI072252, AI078897 and AR42689 (to U.H.v.A.), the Giovanni Armenise-Harvard foundation (to M.I.) and a NIH T32 Training Grant in Hematology (to E.A.M.).

References

1. von Andrian UH, Mempel TR. Homing and cellular traffic in lymph nodes. *Nature Reviews Immunology*. 2003; 3:867–878.
2. Junt T, et al. Subcapsular sinus macrophages in lymph nodes clear lymph-borne viruses and present them to antiviral B cells. *Nature*. 2007; 450:110–114. [PubMed: 17934446]
3. Phan TG, Grigorova I, Okada T, Cyster JG. Subcapsular encounter and complement-dependent transport of immune complexes by lymph node B cells. *Nat Immunol*. 2007; 8:992–1000. [PubMed: 17660822]
4. Carrasco YR, Batista FD. B cells acquire particulate antigen in a macrophage-rich area at the boundary between the follicle and the subcapsular sinus of the lymph node. *Immunity*. 2007; 27:160–171. [PubMed: 17658276]
5. Lyles, DSRC. *Fields Virology*. Howley, PM.; Knipe, DM., editors. Vol. 1. Lippincott Williams & Wilkins; 2007. p. 1363-1408.
6. Hangartner L, Zinkernagel RM, Hengartner H. Antiviral antibody responses: the two extremes of a wide spectrum. *Nat Rev Immunol*. 2006; 6:231–243. [PubMed: 16498452]
7. Probst HC, et al. Histological analysis of CD11c-DTR/GFP mice after in vivo depletion of dendritic cells. *Clin Exp Immunol*. 2005; 141:398–404. [PubMed: 16045728]
8. Purtha WE, Chachu KA, Virgin HWt, Diamond MS. Early B-cell activation after West Nile virus infection requires alpha/beta interferon but not antigen receptor signaling. *J Virol*. 2008; 82:10964–10974. [PubMed: 18786989]
9. Muller U, et al. Functional role of type I and type II interferons in antiviral defense. *Science*. 1994; 264:1918–1921. [PubMed: 8009221]
10. Delemarre FG, Kors N, Kraal G, van Rooijen N. Repopulation of macrophages in popliteal lymph nodes of mice after liposome-mediated depletion. *J Leukoc Biol*. 1990; 47:251–257. [PubMed: 2137849]
11. Chandran K, Sullivan NJ, Felbor U, Whelan SP, Cunningham JM. Endosomal proteolysis of the Ebola virus glycoprotein is necessary for infection. *Science*. 2005; 308:1643–1645. [PubMed: 15831716]
12. Hickman HD, et al. Direct priming of antiviral CD8+ T cells in the peripheral interfollicular region of lymph nodes. *Nat Immunol*. 2008; 9:155–165. [PubMed: 18193049]
13. Brundler MA, et al. Immunity to viruses in B cell-deficient mice: influence of antibodies on virus persistence and on T cell memory. *Eur J Immunol*. 1996; 26:2257–2262. [PubMed: 8814275]

14. Thomsen AR, et al. Cooperation of B cells and T cells is required for survival of mice infected with vesicular stomatitis virus. *Int Immunol.* 1997; 9:1757–1766. [PubMed: 9418136]
15. Asselin-Paturel C, et al. Mouse type I IFN-producing cells are immature APCs with plasmacytoid morphology. *Nat Immunol.* 2001; 2:1144–1150. [PubMed: 11713464]
16. Lund JM, et al. Recognition of single-stranded RNA viruses by Toll-like receptor 7. *Proc Natl Acad Sci U S A.* 2004; 101:5598–5603. [PubMed: 15034168]
17. Iparraguirre A, et al. Two distinct activation states of plasmacytoid dendritic cells induced by influenza virus and CpG 1826 oligonucleotide. *J Leukoc Biol.* 2008; 83:610–620. [PubMed: 18029397]
18. Detje CN, et al. Local type I IFN receptor signaling protects against virus spread within the central nervous system. *J Immunol.* 2009; 182:2297–2304. [PubMed: 19201884]
19. Jung S, et al. In vivo depletion of CD11c(+) dendritic cells abrogates priming of CD8(+) T cells by exogenous cell-associated antigens. *Immunity.* 2002; 17:211–220. [PubMed: 12196292]
20. Maloy KJ, et al. Qualitative and quantitative requirements for CD4+ T cell-mediated antiviral protection. *J Immunol.* 1999; 162:2867–2874. [PubMed: 10072535]
21. Mempel TR, et al. Regulatory T cells reversibly suppress cytotoxic T cell function independent of effector differentiation. *Immunity.* 2006; 25:129–141. [PubMed: 16860762]
22. Whelan SP, Ball LA, Barr JN, Wertz GT. Efficient recovery of infectious vesicular stomatitis virus entirely from cDNA clones. *Proc Natl Acad Sci U S A.* 1995; 92:8388–8392. [PubMed: 7667300]
23. Van Rooijen N, Sanders A. Liposome mediated depletion of macrophages: mechanism of action, preparation of liposomes and applications. *J Immunol Methods.* 1994; 174:83–93. [PubMed: 8083541]
24. Iannacone M, et al. Platelets mediate cytotoxic T lymphocyte-induced liver damage. *Nat Med.* 2005; 11:1167–1169. [PubMed: 16258538]
25. Shao C, Liu M, Wu X, Ding F. Time-dependent expression of myostatin RNA transcript and protein in gastrocnemius muscle of mice after sciatic nerve resection. *Microsurgery.* 2007; 27:487–493. [PubMed: 17596894]
26. Iannacone M, et al. Platelets prevent IFN-alpha/beta-induced lethal hemorrhage promoting CTL-dependent clearance of lymphocytic choriomeningitis virus. *Proc Natl Acad Sci U S A.* 2008; 105:629–634. [PubMed: 18184798]

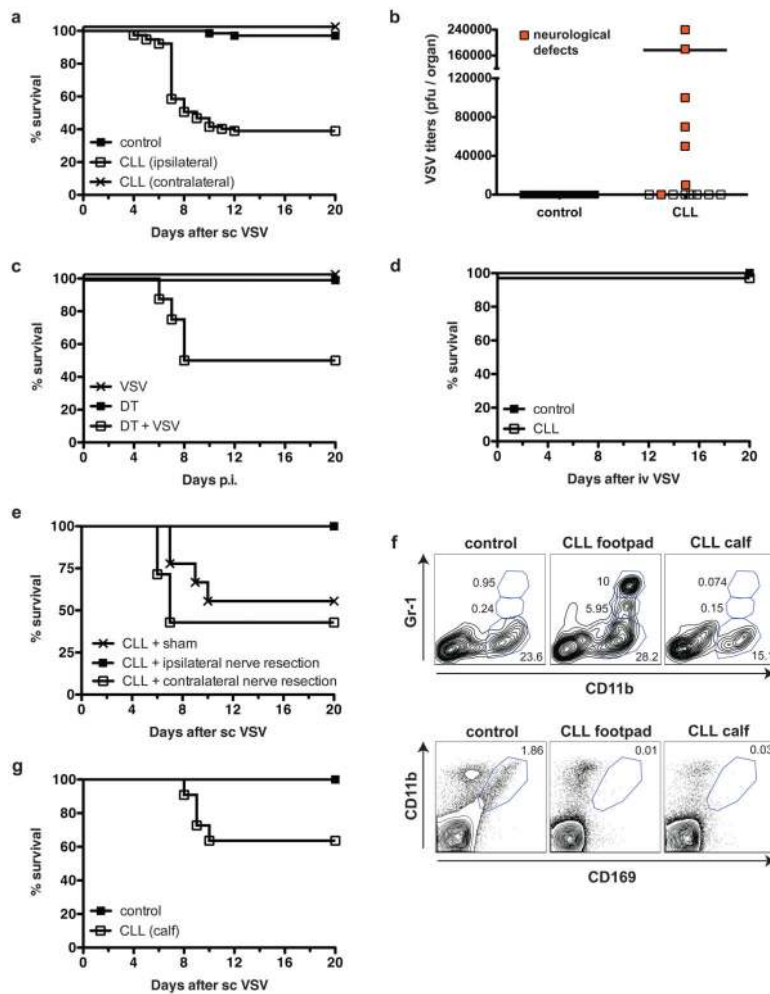


Figure 1. Lymph node macrophages confer resistance to fatal CNS invasion upon peripheral low-dose VSV infection

a. Survival curves of control mice ($n=68$) and mice that received ipsilateral ($n=77$) or contralateral ($n=10$) CLL injection prior to VSV infection. CLL ipsilateral versus control, $P<0.0001$. **b.** VSV titers in the brain of control and CLL-treated mice, 7d after VSV infection. Red squares identify paralytic animals. $P=0.024$. **c.** Survival curves of CD11c-DTR mice ($n=8$); $P=0.0256$. **d.** Survival curves of control and CLL-treated mice after intravenous VSV infection ($n=10$). **e.** Survival curves of CLL-treated VSV infected mice after ipsilateral ($n=10$) or contralateral ($n=7$) sciatic nerve resection. $P=0.007$. **f.** FACS plots of digested footpads (top) and the popliteal LN (bottom) of control and CLL footpad- or calf-injected mice. Numbers represent the percentage of CD45+ cells within each gate. Plots are representative of 2 experiments ($n=3$ mice/experiment). **g.** Survival curves in control ($n=10$) and calf CLL-treated mice ($n=11$). $P=0.0411$.

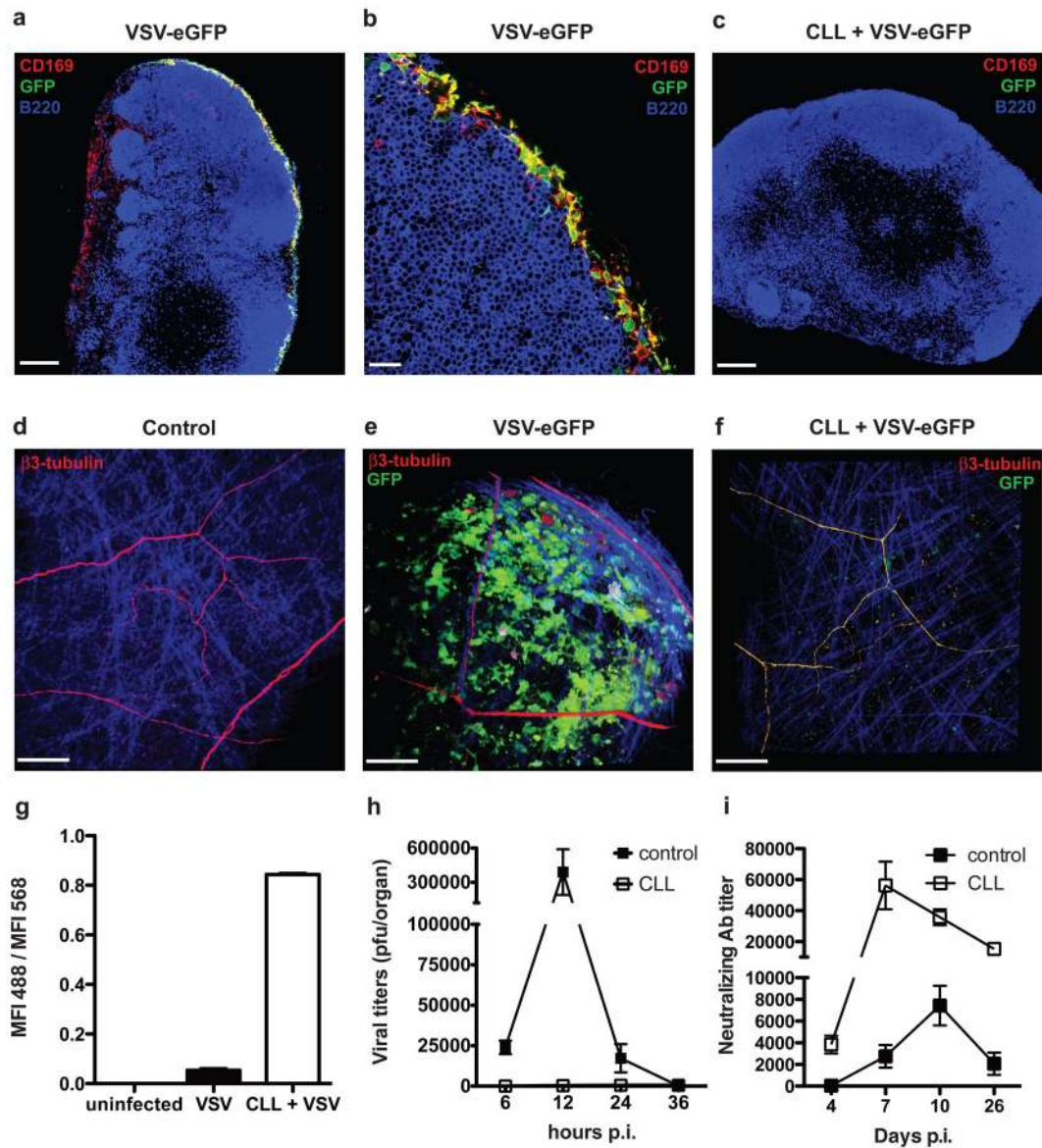


Figure 2. SCS macrophages are the primary targets for lymph-borne VSV and prevent infection of adjacent nerves

a–c, Representative micrographs of macrophage-sufficient (**a,b**) or CLL-treated (**c**) popliteal LNs after VSV-eGFP infection. Scale bars reflect 150 μ m (**a,c**) or 20 μ m (**b**). **d–f**, Representative MP-IVM micrographs of uninfected (**d**) or VSV-eGFP-infected LNs (**e,f**). VSV-eGFP infection of macrophage-sufficient LNs (**e**) induced GFP expression in macrophages but not in nerves (red), whereas nerves in CLL-treated LNs (**f**) expressed GFP (Suppl. Movies 1,2). Scale bars reflect 100 μ m. Blue depicts second harmonic signal from collagen in the LN capsule. **g**, Ratio of mean fluorescent intensities (MFI) in the green (488nm) and red channel (568nm) depicting GFP expression and β 3-tubulin staining, respectively, in peripheral nerves. $n=3$, $P<0.0001$ (VSV versus CLL+VSV). **h**, VSV titers in popliteal LNs of control and CLL-treated mice. $n=4$, $P=0.0010$ (6h), $P<0.0001$ (12h),

$P=0.1043$ (24h), $P=0.0765$ (36h). **i**, Serum neutralizing Ig titers in control and CLL-treated infected mice. $n=4$, $P=0.0053$ (d4), $P=0.0138$ (d7), $P=0.0022$ (d10), $P=0.0054$ (d26).

Author Manuscript

Author Manuscript

Author Manuscript

Author Manuscript

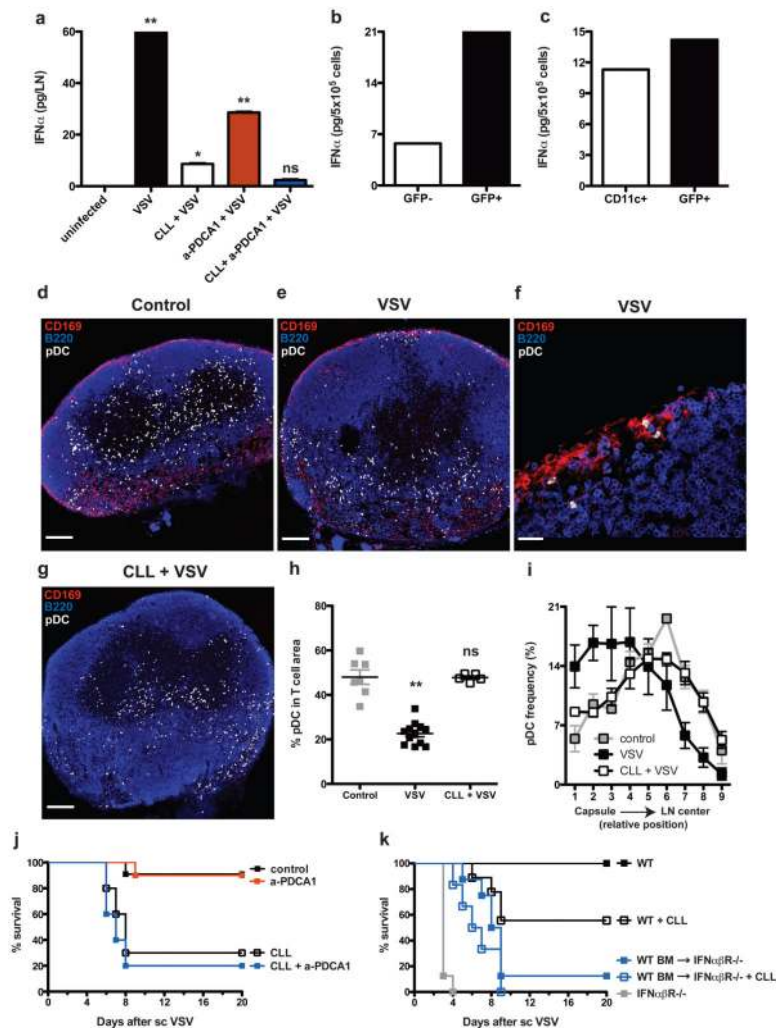


Figure 3. Regulation of VSV-induced IFN-I production by SCS macrophages

a, VSV-induced IFN α production in LNs ($n=3$); *, $P<0.05$, **, $P<0.001$ versus uninfected.

b,c, IFN α concentrations in supernatants of FACS-sorted LN cells after VSV-eGFP infection (Suppl. Fig. 9a,b). Results are from one (of 3) representative experiment. **d–g**,

Micrographs of popliteal LN sections from BM chimeric mice with 30% GFP $^{+}$ pDCs (Suppl. Fig. 10) that were either left untreated (**d**) or sacrificed 8h after VSV infection (**e–g**) without (**e,f**) or with CLL pretreatment (**g**). Scale bars reflect 150 μ m (**d, e, g**) or 20 μ m (**f**). **h**,

pDC frequency in the T cell area ($n=4$ mice/group). **, $P<0.001$ versus control. **i**, Relative

pDC frequency distribution in LNs cross-sections (Suppl. Fig. 12). VSV versus control, $P<0.05$. **j**, Effect of depletion of LN macrophages, pDCs or both on survival upon VSV

infection; a-PDCA1 versus control, ns; CLL versus CLL+a-PDCA1, ns. **i**, Survival curves of

wild-type (WT), IFN $\alpha\beta$ R $^{-/-}$ or irradiated IFN $\alpha\beta$ R $^{-/-}$ mice that were reconstituted with WT BM upon VSV infection. $n=8$. WT BM \rightarrow IFN $\alpha\beta$ R $^{-/-}$ versus WT+CLL, ns; WT BM \rightarrow IFN $\alpha\beta$ R $^{-/-}$ versus IFN $\alpha\beta$ R $^{-/-}$, $P=0.0001$.